Published in final edited form as:

Free Radic Biol Med. 2015 July ; 84: 22–29. doi:10.1016/j.freeradbiomed.2015.02.027.

The NADPH oxidase NOX5 protects against apoptosis in ALK-positive anaplastic large-cell lymphoma cell lines

S. Carnesecchi[a,b], **A.-L. Rougemont**[c], **J.H. Doroshow**[e], **M. Nagy**[b], **S. Mouche**[a], **F. Gumy-Pause**[f], **I. Szanto**[a,d,*]

[a]Department of Cellular Physiology and Metabolism and [b]Department of Pathology and Immunology, University of Geneva, CH-1211 Geneva 4, Switzerland [c]Division of Clinical Pathology and [d]Department of Internal Medicine Specialties, University Hospitals of Geneva, Geneva, Switzerland [e]Center for Cancer Research, National Cancer Institute, National Institutes of Health, Bethesda, MD 20892, USA [f]Department of Pediatrics, Hematology/Oncology Unit, CANSEARCH Research Laboratory, Geneva, Switzerland

Abstract

Reactive oxygen species (ROS) are key modulators of apoptosis and carcinogenesis. One of the important sources of ROS is NADPH oxidases (NOXs). The isoform NOX5 is highly expressed in lymphoid tissues, but it has not been detected in any common Hodgkin or non-Hodgkin lymphoma cell lines. In diverse, nonlymphoid malignant cells NOX5 exerts an antiapoptotic effect. Apoptosis suppression is the hallmark feature of a rare type of lymphoma, termed anaplastic lymphoma kinase-positive (ALK^+) anaplastic large-cell lymphoma (ALCL), and a major factor in the therapy resistance and relapse of ALK^+ ALCL tumors. We applied RT-PCR and Western blot analysis to detect NOX5 expression in three ALK^+ ALCL cell lines (Karpas-299, SR-786, SUP-M2). We investigated the role of NOX5 in apoptosis by small-interfering RNA (siRNA)-mediated gene silencing and chemical inhibition of NOX5 using FACS analysis and examining caspase 3 cleavage in Karpas-299 cells. We used immunohistochemistry to detect NOX5 in ALK^+ ALCL pediatric tumors. NOX5 mRNA was uniquely detected in ALK^+ ALCL cells, whereas cell lines of other lymphoma classes were devoid of NOX5. Transfection of NOX5-specific siRNA and chemical inhibition of NOX5 abrogated calcium-induced superoxide production and increased caspase 3-mediated apoptosis in Karpas-299 cells. Immunohistochemistry revealed focal NOX5 reactivity in pediatric ALK^+ ALCL tumor cells. These results indicate that NOX5-derived ROS contribute to apoptosis blockage in ALK^+ ALCL cell lines and suggest NOX5 as a potential pharmaceutical target to enhance apoptosis and thus to suppress tumor progression and prevent relapse in pediatric ALK^+ ALCL patients that resist classical therapeutic approaches.

*Corresponding author at: Department of Internal Medicine Specialties, University Hospitals of Geneva, Geneva, Switzerland. Fax: +(41 22) 379 5220. ildiko.szanto@unige.ch (I. Szanto).

Appendix A. Supporting information

Supplementary data associated with this article can be found in the online version at http://dx.doi.org/10.1016/j.freeradbiomed.2015.02.027.

Keywords

Reactive oxygen species; NOX5; Anaplastic large-cell lymphoma; Karpas-299; Apoptosis; Free radicals

Anaplastic large-cell lymphoma (ALCL) is a heterogeneous group of aggressive peripheral T cell lymphomas accounting for about 3% of adult and 15% of pediatric non-Hodgkin lymphomas (NHLs) [1,2]. ALCL is characterized by the presence of cohesive sheets of large lymphoid cells of T or null cell phenotype and is distinguished by the expression of the Ki-1/CD30 antigen [3–5]. ALCL is frequently associated with chromosomal translocation, in which the *ALK* gene, encoding an orphan tyrosine kinase receptor, is fused to a variety of other genes. The resulting fused anaplastic lymphoma receptor tyrosine kinase (ALK) is constitutively active and functions as an oncoprotein, triggering uncontrolled cell proliferation and resistance to apoptotic signals [6–10]. ALK mediates its effects through diverse but interconnected and overlapping pathways, including the phosphatidylinositol 3-kinase/AKT/mTOR, the mitogen-activated protein kinase (MAPK/ERK1/2), the phospholipase C-γ (PLC-γ), and the Janus-activated kinase/signal transducer and activator of transcription pathways [6,11,12]. These pathways mediate antiapoptotic, mitogenic, or inflammatory signals. One of the common regulatory mechanisms involved in all these pathways is the production of reactive oxygen species (ROS). ROS generation can be related to both physiological cell function and cell toxicity, depending on the amount, the source, and the intracellular localization of ROS production. Specifically, ROS can act as second messengers in signaling cascades, promoting cell growth and differentiation, and/or perform as apoptotic or antiapoptotic signals [13]. The only known enzymes solely dedicated to ROS generation are NADPH oxidases (NOXs). Over the past 15 years a number of ROS-producing NADPH oxidase isoforms have been identified, but their physiological and pathological roles are still largely unexplored [14–18]. NOX5 is a special member of the NOX enzyme family, as it is expressed in humans but has no rodent homolog, severely hampering opportunities to investigate its function in a physiological context. High NOX5 mRNA expression is detected in the germinal centers of spleen and lymph nodes, regions that are rich in B and T cells; however, NOX5 is absent from circulating lymphocytes [19]. Another striking feature of NOX5 is that its expression is upregulated in some cancers and in various transformed cancer cell lines, but no strong NOX5 expression has been reported in hematopoietic or lymphoid cancer cells except for a low level of expression in hairy cell leukemia [20,21]. In prostate cancer cells, inhibition of NOX5-derived ROS production resulted in enhanced apoptosis, suggesting that NOX5 may be an antiapoptotic molecule [20]. Resistance to proapoptotic signaling is a characteristic feature of ALCL resulting in aggressive growth [22]. In general, ALCLs have a good prognosis; however, about 20–30% of patients relapse owing to the survival of residual, conventional therapy-resistant tumor cells [6,23]. Thus, identifying molecules that activate additional antiapoptotic pathways is of significant clinical interest for the treatment of ALCL.

Our study revealed NOX5 expression in three independent ALK^+ ALCL cell lines and demonstrates that NOX5 depletion results in enhanced apoptosis *via* the activation of the caspase 3 pathway. To confirm the clinical potential of our data, we identified a number of

NOX5-positive cells in ALCL pediatric tumors. Taken together, our results suggest a role for NOX5 in the apoptosis-resistant phenotype of ALK^+ ALCL cell lines *in vitro* and may indicate that it is involved in the aggressive tumor growth and apoptosis resistance that are hallmark features of ALCL malignancies.

Materials and methods

Cell culture

Karpas-299, SR-786, and SUP-M2 cells were purchased from the German National Resource Center for Biological Material (Braunschweig, Germany) and were cultured in RPMI 1640 medium supplemented with 10% fetal calf serum and 100 U/ml penicillin and 100 μg/ml streptomycin. Ionomycin, melittin (Sigma, Busch, Switzerland), and thapsigargin (Calbiochem, Darmstadt, Germany) were diluted in dimethyl sulfoxide (DMSO).

Small interfering RNA (siRNA) transfections

SiRNA duplex oligonucleotides specific for the human NOX5 mRNA were designed based upon published sequence (NM_024505) and were as follows: siRNA sense, 5′-GGUGGACUUUAUCUGGAUCtt-3′; siRNA antisense, 5′-GAUCCAGAUAAAGUCCACCtt-3′ (Ambion, Cambridgeshire, UK). Control scrambled siRNA sequence was 5′-AATTC-TCCGAACGTGTCACGT-3′ (Xeragon, Cologne, Germany). Transfections were performed using an RNAiFect transfection kit following the manufacturer's protocol (Qiagen, Basel, Switzerland). Cells were harvested for subsequent analysis at 24 or 48 h after transfection.

Reverse transcription and polymerase chain reaction

Total RNA was prepared using Trizol reagent (Invitrogen, Basel, Switzerland). Two micrograms of DNA-free RNA was reverse transcribed using Superscript II reverse transcriptase (Invitrogen). PCR was carried out using TaqDNA polymerase (Qiagen). Primers specific for the different regions of human NOX5 and β-actin are listed in Supplementary Table S1. cDNAs of human tonsil, fetal thymus, spleen, and testis were purchased from Clontech (Mountain View, CA, USA).

Detection of ROS production

Forty-eight hours after transfection, 0.5×10^5 Karpas-299 cells were placed in a 96-well microplate. ROS production was measured by chemiluminescence in the presence of 5-amino-2, 3-dihydro-1,4-phthalazinedione (luminol; Sigma) using a thermostatically (37 °C) controlled luminometer (Fluoroskan Ascent FL, Catalys, Wallisellen, Switzerland). Cells were incubated in Hanks' balanced salt solution supplemented with luminol (60 μM) and horseradish peroxidase (0.5 U/ml) under basal conditions or in the presence of ionomycin (1 μM) or thapsigargin (6 μM). Chemiluminescence was monitored continuously for 30 min. Background fluorescence was measured in the absence of cells.

Cell proliferation measurements

Karpas-299 cells transfected with scrambled or NOX5-specific siRNA were seeded into 24-well plates at a density of 1×10^6 cells per well and stained with trypan blue dye (Invitrogen). Direct cell counts were performed by optical microscopy or by Countess automated cell counter (Invitrogen).

Apoptosis detection

To distinguish live, apoptotic, and necrotic cells, Karpas-299 cells transfected with scrambled or siNOX5 siRNAs were washed in phosphate-buffered saline and stained with 7-amino actinomycin D (7-AAD, 0.3 μg/ml) and analyzed immediately in a flow cytometer (Becton–Dickinson Immunocytometry Systems). Data from 10,000 events per sample were collected and analyzed using the CellQuest analysis program (BD Biosciences). The regions representing alive, apoptosis, and late apoptosis/necrosis were defined according to the 7-AAD fluorescence (FL3-negative, -dim, and -bright, respectively) combined with cell morphology (FSH) [24]. Unstained fixed cells were used as negative controls.

Western blot

Karpas-299 cells (1×10^6) were lysed in RIPA NP-40 buffer (300 mM NaCl, 2% NP-40, 0.2% SDS, 1% deoxycholic acid, 100 mM Tris–HCl, pH 7.4, 0.5 mM EDTA, 3 mM orthovanadate, 10 mM NaF, and a cocktail of protease inhibitors (Roche, Mannheim, Germany). Cells were centrifuged for 10 min at 13,000 *g.* Supernatants were collected and proteins were separated by SDS–PAGE and electrophoretically transferred to nitrocellulose membrane. Nonspecific binding was blocked using 4 mg/ml polyvinyl alcohol (BASF AG, Wädenswil, Switzerland) in Tris-buffered saline (4 mM Tris base, 100 mM NaCl, pH 7.5) and 0.1% Tween. Membranes were incubated with the anti-NOX5 rabbit polyclonal antibody (generated against the recombinant fragment of human NOX5 (NP_078781) encoding amino acids 199–240, a gift from Dr. Eric Ogier-Denis, INSERM Unité 479, Faculté de Médecine Xavier Bichat, Paris, France) at a dilution of 1/1000 at 4 °C overnight. Commercial antibodies are listed in Supplementary Table S2. Membranes were then washed and incubated for 1 h in the presence of horseradish peroxidase (HRP)-conjugated goat anti-mouse or anti-rabbit antibody at a dilution of 1/3000 (Sigma–Aldrich). The immune complexes were visualized using Supersignal West Dura chemiluminescent substrate (Perbio Science, Lausanne, Switzerland) and the intensity of the bands was measured in a Geldoc image analyzer (PXi multifunction gel documentation; Syngene, Cambridge, UK).

Tumor samples

Paraffin-embedded biopsy or surgical samples from three pediatric patients, originally obtained for diagnostic purposes, were retrieved from the archives of the Division of Clinical Pathology of the Geneva University Hospitals. Patients' characteristics are summarized in Table 1. The study has been accepted by the Ethics Committee of the Geneva University Hospitals.

Immunohistochemistry

Formalin-fixed, paraffin-embedded tissue sections (4 μm thick) were analyzed by immunohistochemistry using a mouse monoclonal antibody specific for NOX5 [25], ALK (Dako M7195), or CD30 (Ventana Medical Systems, Tucson, AZ, USA, 790–2926). Staining was performed using the automated Ventana Discovery system for NOX5 and ALK or Ventana BenchMark XT system for CD30 (Ventana Medical Systems). Ventana reagents were used for all procedures. Briefly, slides were heated with cell conditioning solution for 36 min, for ALK and NOX5 antibodies, or for 64 min for CD30 (CC1; Tris-based buffer, pH 8.4). Primary antibodies were used at a dilution of 1/1000 or 1/50 for NOX5 or ALK, respectively. CD30 was used according to the manufacturer's instructions. Detection of primary antibodies was carried out using the amplified DAB detection kit based on the conversion of diaminobenzidine to a dye with multimeric horseradish peroxidase.

Data presentation and statistical analysis

Data are presented as means ± SEM. Statistical analysis was carried out using unpaired Student's *t* test; $p < 0.05$ was considered significant.

Results

Distribution of NOX5 mRNA in human lymphoma cell lines

NOX5 mRNA was strongly expressed in three different ALK^+ ALCL cell lines (SR-786, SUP-M2, and Karpas-299). Other lymphoma cell lines representing NHL (HDLM2, L428, L591) and Hodgkin-type lymphomas, including the T cell lymphoma CEM and Jurkat, the Burkitt lymphoma Raji, and the large-cell lymphoma IM9 cells, were devoid of NOX5 (Fig. 1A). NOX5 is activated by Ca^{2+} binding through its EF-hand motifs situated in the N-terminus of the molecule [19,26,27]. RT-PCR amplification of a 1796-bp part of the NOX5 transcript containing the region of the four EF hands demonstrated the presence of this crucial activation domain of NOX5 in all ALCL cell lines (Fig. 1B). The N-terminal part of NOX5 can undergo alternative splicing giving rise to different isoforms. The isoforms with the highest expression levels are termed α and β and are present in lymphoid tissues and testis, respectively [19]. In line with their lymphoid origin, all three ALCL cell lines expressed the NOX5α isoform as demonstrated by RT-PCR analysis using isoform-specific primers (Fig. 1C). ALCL cells were devoid of NOX5β (data not shown).

Expression of NOX5 in ALK^+ ALCL tumor samples

To examine the potential clinical role of NOX5 in ALCL development, we used immunohistochemical analysis to detect NOX5 in ALK^+ ALCL pediatric tumor samples obtained at diagnosis, before therapy. The specificity of the NOX5 antibody has been demonstrated in a previous publication [25] and has been validated in the frame of this experiment, again using wild-type and NOX5-overexpressing HEK293 cells [19] (a generous gift from K.-H. Krause, University of Geneva, Geneva, Switzerland) and on uterine sections (Supplementary Fig. S1). Hematoxylin and eosin (HE) staining of the tumor samples revealed nodular infiltration with sheets of highly pleomorphic polygonal cells presenting large, vesicular, irregular, convoluted nuclei; variably prominent nucleoli; and

abundant eosinophilic cytoplasm. Occasional tumor cells showed a typical eccentric horseshoe-shaped nucleus. Mitoses and apoptotic bodies were numerous. Tumor cells were intermingled with plasma cells and small lymphocytes (Fig. 2; HE). Sections from all three tumors showed a large number of $CD30^+$ cells with characteristic membranous and Golgi staining (Fig. 2; CD30). Patients 1 and 3 displayed strong and diffuse ALK staining, whereas reactivity was less intense in patient 2 (Fig. 2; ALK). Focal reactivity to T cell markers and EMA was also observed (see patients' characteristics, Table 1). A t(2;5)(p23;q35) (*NPM1*/*ALK*) translocation was found in patient 1; RT-PCR was not performed in the other two patients. Concerning NOX5, we observed faint but distinct staining in some of the tumor cells, with a nuclear signal in patient 1 and faint and focal cytoplasmic staining in patient 2. A minority of tumor cells showed barely discernible cytoplasmic staining in patient 3. In addition to tumor cells, plasma cells showed NOX5 cytoplasmic reactivity (Fig. 2; NOX5).

NOX5 depletion hampers ROS production and increases apoptosis in Karpas-299 cells

To shed light on the potential involvement of NOX5 in a certain aspect of ALCL tumorigenesis, we applied siRNA-mediated gene knockdown in Karpas-299 cells and investigated its effect on superoxide generation, cell proliferation, and apoptosis. Transfection of NOX5-specific siRNA significantly decreased NOX5 mRNA and protein expression (Figs. 3A and B). In parallel, NOX5 depletion abrogated superoxide generation induced by the calcium-mobilizing agents ionomycin and thapsigargin as demonstrated by luminol assay (Figs. 3C–E). siRNA-mediated NOX5 knockdown led to a significant decrease in the number of viable cells after 24 and 48 h of transfection as measured by trypan blue exclusion assay (20 and 31.2% at 24 and 48 h, respectively; Fig. 4A). These results were confirmed by staining the cells with 7-AAD and analyzing them by fluorescence-activated cell sorting (FACS). Indeed, NOX5 depletion induced a significant decrease in viable cells and an increase in apoptotic cells after both 24 and 48 h of transfection (Figs. 4B and C). This finding was also sustained by enhanced activation (cleavage) of caspase 3, a major mediator of cell death [28]. In fact, after 48 h of NOX5-specific siRNA transfection Karpas-299 cells displayed a threefold elevation in cleaved caspase 3 levels (Figs. 4D and E).

Pharmacological inhibition of NOX5 induces apoptosis in Karpas-299 cells

To confirm the antiapoptotic role of NOX5 implied by the siRNA-mediated gene knockdown experiments, we treated Karpas-299 cells with melittin, a calcium chelator and thus an inhibitor of NOX5 activity [27]. Melittin treatment (0.5, 2, and 3.5 μg/ml) led to a dose-dependent increase in apoptosis at 2 and 3.5 μg/ml by 72 h of treatment accompanied by an induction of caspase 3 cleavage (Figs. 4E and F).

Discussion

In the present study we used both a genetic depletion approach and chemical inhibition to establish NOX5 as a key apoptosis suppressor in ALK^+ ALCL cell lines in vitro and revealed that the antiapoptotic effect of NOX5 is mediated through the inhibition of caspase 3 cleavage. In addition, using immunohistochemical analysis we demonstrated faint NOX5

expression in a subset of tumor cells in histological sections derived from pediatric ALK^+ ALCL patients.

ALCL is an aggressive CD30-positive T or null cell NHL that was described 30 years ago by Stein et al. [3]. This lymphoid neoplasia is characterized by malignant cells displaying eccentric horseshoe- or kidney-shaped nuclei (hallmark cells). These hallmark cells frequently exhibit a chromosomal translocation involving the *ALK* gene resulting in the constitutive activation of ALK (ALK^+ ALCL). In children, ALCL is almost exclusively ALK^+, whereas in adults ALK^+ ALCL represents only about 50% of ALCL cases [62].

In 75% of pediatric ALCL, the disease is already disseminated at diagnosis, with a high incidence of nodal and extranodal involvement (skin, lung, bone, and liver). In the past, a wide range of anthracycline based-chemotherapy strategies has been implemented; however, no improvement in the failure rate of 25–30% has been realized. Recurrent disease is frequently chemosensitive, and 50 to 75% of children with relapse can be cured with autologous or allogeneic hematopoietic stem cell transplantation. Unfortunately, these intensive treatments may be highly toxic with severe short- or long-term side effects (reviewed in [29]). It is obvious that new therapeutic strategies are required to improve the outcome of ALCL and to decrease toxicity. Indeed, currently, numerous clinical trials with anti-CD30 antibodies or ALK inhibitors are under way, with interesting preliminary results (reviewed in [29–31]). However, therapeutic responses to ALK-targeted drugs are limited by acquired drug resistance owing to novel mutations in the *ALK* gene or to activation of alternative proliferative signals during treatment [32,33]. Thus, significant research efforts are currently being devoted to the identification of novel therapeutic targets to inhibit other, additional antiapoptotic pathways and thus to induce a higher degree of tumor cell death [34]. Indeed, ALCL cells are characterized by a low apoptotic rate, and one of the perceived causes of therapeutic resistance is the survival and proliferation of residual tumor cells [6,23].

One of the major apoptosis-regulating factors is the production of ROS derived from various NOX enzymes [35]. Specifically, the NOX5 isoform has been linked to tumorigenesis and apoptosis inhibition in diverse types of cancer [17]. Our data reveal a highly specific expression of NOX5α, the lymphoid isoform of NOX5, in three different ALK^+ ALCL cell lines. NOX5 is known to exist in five different isoforms, the most abundant being the α (lymphoid) and the β (testis) isoforms [17]. The two major isoforms have almost identical ROS-producing capacity, and currently no biochemical or physiological differences between them have been documented [36]. We applied immunohistochemical detection of NOX5 to identify NOX5-experssing cells in pediatric ALK^+ ALCL biopsies. The pattern of immunohistochemical reactivity to NOX5 in pediatric ALK^+ ALCL samples was faint and focal, displaying either a nuclear or a cytoplasmic reactivity. These results are in line with a recent study demonstrating the presence of NOX5 in the cytosol and/or the nucleus in renal proximal tubule cells derived from patients with hypertension, in leukemia cells, in endocardial and vascular endothelial cells, in vascular smooth muscle cells, and in prostate cancer cells [20,37–39]. The precise physiopathological significance of different NOX5 intracellular localization is currently unknown. Nuclear ROS production might be involved in the modulation of mitogenic gene transcription, nuclear MAPK activation, and/or

nucleoplasmic calcium release from the nuclear T-tubule system [39]. The characterization of the importance of nuclear NOX5-derived superoxide production in these processes was out of the scope of the current study but will constitute a worthy topic for further investigations.

Signal intensity obtained in the ALK^+ ALCL samples was insufficient to be considered as a diagnostic or prognostic aid in clinical practice. Developing novel, more robust NOX5 antibodies will be required to resolve this technical issue and to obtain staining adequate for clinicopathological application. However, our investigations provided evidence for the presence of NOX5 protein in a subset of ALCL tumor cells, suggesting a role for NOX5 at defined steps in ALK^+ ALCL tumorigenesis. The current study did not aim to unravel the precise mechanisms driving NOX5 expression/upregulation in these tumor cells; such studies will require a more thorough approach employing an extensive ALCL sample collection and more detailed methods, e.g., a comparative expression profile of tumors with different histopathological features, clinical staging, and outcome. Instead, to understand the underlying mechanisms that link NOX5 to ALCL tumorigenesis, we investigated the molecular signaling pathways modulated by NOX5-derived ROS in Karpas-299 cells, an ALK^+ ALCL model cell line *in vitro*.

ROS have been demonstrated to foster tumorigenesis by stimulating antiapoptotic pathways [40,41]. In particular, apoptosis blockage through the oxidative inhibition of caspase 3 cleavage is a crucial factor in ALCL tumor formation [22,42]. Caspase 3 is a cysteine protease that acts as the final executor of the apoptotic process for both intrinsic and extrinsic apoptotic signals. Caspase 3 is activated through the cleavage of the inactive procaspase into two molecules that will then associate to form a heterotetramer. The active site of this heterotetramer molecule possesses redox-sensitive cysteine and histidine residues [43–45]. Oxidation of these residues by ROS results in diminished caspase 3 apoptotic activity [46,47]. Concerning the sources of ROS, the mitochondria and NOX enzymes are the subjects of most investigations [35,48,49]. In addition, recent studies revealed a potential role for bioactive metabolites of lipoxygenase enzymes in tumorigenesis, more specifically in ALK^+ ALCL development [50,51]. Current views of ROS generation in apoptosis regulation suggest a complex and vastly interconnected network between these three major cellular sources of ROS. Indeed, mitochondrial ROS can stimulate NOX activity, which in turn can regulate mitochondrial function through redox modification of mitochondrial proteins [52]. Of particular interest is that the proapoptotic function of mitochondrial cytochrome *c*, a major inducer of the caspase 3-mediated apoptotic cascade, is suppressed by ROS [53]. Lipoxygenase enzymes produce diverse types of bioactive lipid signaling molecules, e.g., leukotrienes that can induce ROS production by NOX enzymes and modulate their effects on apoptosis [54]. In ALCL cell lines in particular, inhibition of the leukotriene B4 receptor or treating cells with a lipoxygenase enzyme inhibitor led to enhanced caspase 3 cleavage and apoptosis [50,51]. Our results demonstrate that NOX5-derived ROS play a key role in apoptosis suppression exerting effects through inhibition of caspase 3 cleavage. Whether, and how, NOX5-derived ROS may crosstalk with other cellular ROS sources is a worthy topic meriting further investigations in future experiments.

NOX5 produces ROS in a Ca^{2+}-dependent manner that is subject to regulation by protein kinase C- and MAPK-mediated phosphorylation to achieve Ca^{2+} sensitivity relevant to physiological intracellular calcium concentrations [19,27,55,56]. Ca^{2+}-induced signaling events are key components in the control of cellular apoptosis [57]. Disturbed Ca^{2+} homeostasis in ALCL tumors is suggested by several lines of evidence. Indeed, the mutant ALK induces calcium mobilization from endoplasmic reticulum stores through constitutive activation of PLC-γ and the production of inositol triphosphate [6,12,58,59]. In addition, ALCL cell lines and tumors display upregulation of diverse calcium-binding proteins [60]. Our results demonstrated NOX5-dependent Ca^{2+}-induced ROS production in Karpas-299 cells. These data, taken together with the enhanced rate of apoptosis observed in NOX5-depleted cells, suggest that NOX5 is a link between pathological Ca^{2+} release, ROS production, and apoptosis; hence, NOX5 may be a key facilitator of ALCL tumorigenesis.

Our study demonstrates the participation of NOX5 in ALK^+ ALCL cell line apoptosis resistance in vitro and suggests its involvement in pediatric ALCL tumor pathogenesis in patients. Owing to the frequent onset of acquired resistance observed during ALK-targeted therapy, the identification of additional pharmacological targets still remains the topic of intensive research efforts [34,61]. In this respect, NOX5 may represent a novel and promising candidate for the development of a supplementary approach to treating ALK^+ ALCLs, most notably those most challenging cases that are resistant to traditional therapeutic means.

Supplementary Material

Refer to Web version on PubMed Central for supplementary material.

Acknowledgments

We thank Nathalie Lin-Marq (University of Geneva) for excellent technical help. This work was supported by a grant from the Fondation Georges Lemaitre, Geneva, Switzerland, allocated to I.S.

References

[1]. Ferreri AJ; Govi S; Pileri SA; Savage KJ Anaplastic large cell lymphoma, ALK-positive. Crit. Rev. Oncol. Hematol 83:293–302; 2012. [PubMed: 22440390]

[2]. Ferreri AJ; Govi S; Pileri SA; Savage KJ Anaplastic large cell lymphoma, ALK-negative. Crit. Rev. Oncol. Hematol 85:206–215; 2013. [PubMed: 22789917]

[3]. Stein H; Mason DY; Gerdes J; O'Connor N; Wainscoat J; Pallesen G; Gatter K; Falini B; Delsol G; Lemke H; et al. The expression of the Hodgkin's disease associated antigen Ki-1 in reactive and neoplastic lymphoid tissue: evidence that Reed–Sternberg cells and histiocytic malignancies are derived from activated lymphoid cells. Blood 66:848–858; 1985. [PubMed: 3876124]

[4]. Harris NL; Jaffe ES; Stein H; Banks PM; Chan JK; Cleary ML; Delsol G; De Wolf-Peeters C; Falini B; Gatter KC; et al. A revised European–American classification of lymphoid neoplasms: a proposal from the International Lymphoma Study Group. Blood 84:1361–1392; 1994. [PubMed: 8068936]

[5]. Morris SW; Kirstein MN; Valentine MB; Dittmer KG; Shapiro DN; Saltman DL; Look AT Fusion of a kinase gene, ALK, to a nucleolar protein gene, NPM, in non-Hodgkin's lymphoma. Science 263:1281–1284; 1994. [PubMed: 8122112]

[6]. Pulford K; Morris SW; Turturro F Anaplastic lymphoma kinase proteins in growth control and cancer. J. Cell. Physiol 199:330–358; 2004. [PubMed: 15095281]

[7]. Inghirami G; Pileri SA Anaplastic large-cell lymphoma. Semin. Diagn. Pathol 28:190–201; 2011. [PubMed: 21850985]

[8]. Fiorani C; Vinci G; Sacchi S; Bonaccorsi G; Artusi T Primary systemic anaplastic large-cell lymphoma (CD30+): advances in biology and current therapeutic approaches. Clin. Lymphoma 2:29–37; 2001. [PubMed: 11707867]

[9]. Barreca A; Lasorsa E; Riera L; Machiorlatti R; Piva R; Ponzoni M; Kwee I; Bertoni F; Piccaluga PP; Pileri SA; Inghirami G Anaplastic lymphoma kinase in human cancer. J. Mol. Endocrinol 47:R11–23; 2011. [PubMed: 21502284]

[10]. Chiarle R; Gong JZ; Guasparri I; Pesci A; Cai J; Liu J; Simmons WJ; Dhall G; Howes J; Piva R; Inghirami G NPM-ALK transgenic mice spontaneously develop T-cell lymphomas and plasma cell tumors. Blood 101:1919–1927; 2003. [PubMed: 12424201]

[11]. Chang F; Lee JT; Navolanic PM; Steelman LS; Shelton JG; Blalock WL; Franklin RA; McCubrey JA Involvement of PI3K/Akt pathway in cell cycle progression, apoptosis, and neoplastic transformation: a target for cancer chemotherapy. Leukemia 17:590–603; 2003. [PubMed: 12646949]

[12]. Bai RY; Ouyang T; Miething C; Morris SW; Peschel C; Duyster J Nucleophosmin-anaplastic lymphoma kinase associated with anaplastic large-cell lymphoma activates the phosphatidylinositol 3-kinase/Akt antiapoptotic signaling pathway. Blood 96:4319–4327; 2000. [PubMed: 11110708]

[13]. Sauer H; Neukirchen W; Rahimi G; Grunheck F; Hescheler J; Wartenberg M Involvement of reactive oxygen species in cardiotrophin-1-induced proliferation of cardiomyocytes differentiated from murine embryonic stem cells. Exp. Cell Res 294:313–324; 2004. [PubMed: 15023522]

[14]. Krause KH Tissue distribution and putative physiological function of NOX family NADPH oxidases. Jpn. J. Infect. Dis 57:S28–29; 2004. [PubMed: 15507765]

[15]. Cheng G; Cao Z; Xu X; van Meir EG; Lambeth JD Homologs of gp91phox: cloning and tissue expression of Nox3, Nox4, and Nox5. Gene 269:131–140; 2001. [PubMed: 11376945]

[16]. Lambeth JD NOX enzymes and the biology of reactive oxygen. Nat. Rev. Immunol 4:181–189; 2004. [PubMed: 15039755]

[17]. Bedard K; Krause KH The NOX family of ROS-generating NADPH oxidases: physiology and pathophysiology. Physiol. Rev 87:245–313; 2007. [PubMed: 17237347]

[18]. Bedard K; Jaquet V; Krause KH NOX5: from basic biology to signaling and disease. Free Radic. Biol. Med 52:725–734; 2012. [PubMed: 22182486]

[19]. Banfi B; Molnar G; Maturana A; Steger K; Hegedus B; Demaurex N; Krause KH A Ca^{2+}-activated NADPH oxidase in testis, spleen, and lymph nodes. J. Biol. Chem 276:37594–37601; 2001. [PubMed: 11483596]

[20]. Brar SS; Corbin Z; Kennedy TP; Hemendinger R; Thornton L; Bommarius B; Arnold RS; Whorton AR; Sturrock AB; Huecksteadt TP; Quinn MT; Krenitsky K; Ardie KG; Lambeth JD; Hoidal JR NOX5 NAD(P)H oxidase regulates growth and apoptosis in DU 145 prostate cancer cells. Am. J. Physiol. Cell Physiol 285:C353–369; 2003. [PubMed: 12686516]

[21]. Kamiguti AS; Serrander L; Lin K; Harris RJ; Cawley JC; Allsup DJ; Slupsky JR; Krause KH; Zuzel M Expression and activity of NOX5 in the circulating malignant B cells of hairy cell leukemia. J. Immunol 175: 8424–8430; 2005. [PubMed: 16339585]

[22]. Desjobert C; Renalier MH; Bergalet J; Dejean E; Joseph N; Kruczynski A; Soulier J; Espinos E; Meggetto F; Cavaille J; Delsol G; Lamant L MiR-29a down-regulation in ALK-positive anaplastic large cell lymphomas contributes to apoptosis blockade through MCL-1 overexpression. Blood 117:6627–6637; 2011. [PubMed: 21471522]

[23]. Schnell R; Barth S; Diehl V; Engert A Hodgkin's disease. Future treatment strategies: fact or fiction? Bailliere's Clin. Haematol 9:573–593; 1996.

[24]. Philpott NJ; Turner AJ; Scopes J; Westby M; Marsh JC; Gordon-Smith EC; Dalgleish AG; Gibson FM The use of 7-amino actinomycin D in identifying apoptosis: simplicity of use and broad spectrum of application compared with other techniques. Blood 87:2244–2251; 1996. [PubMed: 8630384]

[25]. Antony S; Wu Y; Hewitt SM; Anver MR; Butcher D; Jiang G; Meitzler JL; Liu H; Juhasz A; Lu J; Roy KK; Doroshow JH Characterization of NADPH oxidase 5 expression in human tumors

and tumor cell lines with a novel mouse monoclonal antibody. Free Radic. Biol. Med 65:497–508; 2013. [PubMed: 23851018]

[26]. Jagnandan D; Church JE; Banfi B; Stuehr DJ; Marrero MB; Fulton DJ Novel mechanism of activation of NADPH oxidase 5: calcium sensitization via phosphorylation. J. Biol. Chem 282:6494–6507; 2007. [PubMed: 17164239]

[27]. Banfi B; Tirone F; Durussel I; Knisz J; Moskwa P; Molnar GZ; Krause KH; Cox JA Mechanism of Ca^{2+} activation of the NADPH oxidase 5 (NOX5). J. Biol. Chem 279:18583–18591; 2004. [PubMed: 14982937]

[28]. Zhan Y; van de Water B; Wang Y; Stevens JL The roles of caspase-3 and bcl-2 in chemically-induced apoptosis but not necrosis of renal epithelial cells. Oncogene 18:6505–6512; 1999. [PubMed: 10597253]

[29]. Lowe EJ; Gross TG Anaplastic large cell lymphoma in children and adolescents. Pediatr. Hematol. Oncol 30:509–519; 2013. [PubMed: 23758281]

[30]. Perini GF; Pro B Brentuximab vedotin in CD30+ lymphomas. Biol. Ther 3:15–23; 2013. [PubMed: 24392301]

[31]. Mologni L Inhibitors of the anaplastic lymphoma kinase. Expert Opin. Invest. Drugs 21:985–994; 2012.

[32]. Lovly CM; Pao W Escaping ALK inhibition: mechanisms of and strategies to overcome resistance. Sci. Transl. Med 4:120ps2; 2012.

[33]. Katayama R; Shaw AT; Khan TM; Mino-Kenudson M; Solomon BJ; Halmos B; Jessop NA; Wain JC; Yeo AT; Benes C; Drew L; Saeh JC; Crosby K; Sequist LV; Iafrate AJ; Engelman JA Mechanisms of acquired crizotinib resistance in ALK-rearranged lung cancers. Sci. Transl. Med 4:120ra17; 2012.

[34]. Merkel O; Hamacher F; Sifft E; Kenner L; Greil R Novel therapeutic options in anaplastic large cell lymphoma: molecular targets and immunological tools. Mol. Cancer Ther 10:1127–1136; 2011. [PubMed: 21712478]

[35]. Block K; Gorin Y Aiding and abetting roles of NOX oxidases in cellular transformation. Nat. Rev. Cancer 12:627–637; 2012. [PubMed: 22918415]

[36]. Pandey D; Patel A; Patel V; Chen F; Qian J; Wang Y; Barman SA; Venema RC; Stepp DW; Rudic RD; Fulton DJ Expression and functional significance of NADPH oxidase 5 (Nox5) and its splice variants in human blood vessels. Am. J. Physiol. Heart Circ. Physiol 302:H1919–1928; 2012. [PubMed: 22427510]

[37]. Yu P; Han W; Villar VA; Yang Y; Lu Q; Lee H; Li F; Quinn MT; Gildea JJ; Felder RA; Jose PA Unique role of NADPH oxidase 5 in oxidative stress in human renal proximal tubule cells. Redox Biol 2:570–579; 2014. [PubMed: 24688893]

[38]. El Jamali A; Valente AJ; Lechleiter JD; Gamez MJ; Pearson DW; Nauseef WM; Clark RA Novel redox-dependent regulation of NOX5 by the tyrosine kinase c-Abl. Free Radic. Biol. Med 44:868–881; 2008. [PubMed: 18160052]

[39]. Ahmarani L; Avedanian L; Al-Khoury J; Perreault C; Jacques D; Bkaily G Whole-cell and nuclear NADPH oxidases levels and distribution in human endocardial endothelial, vascular smooth muscle, and vascular endothelial cells. Can. J. Physiol. Pharmacol 91:71–79; 2013. [PubMed: 23368419]

[40]. Hussain SP; Hofseth LJ; Harris CC Radical causes of cancer. Nat. Rev. Cancer 3:276–285; 2003. [PubMed: 12671666]

[41]. Sainz RM; Lombo F; Mayo JC Radical decisions in cancer: redox control of cell growth and death. Cancers 4:442–474; 2012. [PubMed: 24213319]

[42]. Oyarzo MP; Drakos E; Atwell C; Amin HM; Medeiros LJ; Rassidakis GZ Intrinsic apoptotic pathway in anaplastic large cell lymphoma. Hum. Pathol 37:874–882; 2006. [PubMed: 16784988]

[43]. Arends MJ; Wyllie AH Apoptosis: mechanisms and roles in pathology. Int. Rev. Exp. Pathol 32:223–254; 1991. [PubMed: 1677933]

[44]. Cohen GM Caspases: the executioners of apoptosis. Biochem. J 326:1–16; 1997. [PubMed: 9337844]

[45]. Grutter MG Caspases: key players in programmed cell death. Curr. Opin. Struct. Biol 10:649–655; 2000. [PubMed: 11114501]

[46]. Ueda S; Masutani H; Nakamura H; Tanaka T; Ueno M; Yodoi J Redox control of cell death. Antioxid. Redox Signaling 4:405–414; 2002.

[47]. Circu ML; Aw TY Reactive oxygen species, cellular redox systems, and apoptosis. Free Radic. Biol. Med 48:749–762; 2010. [PubMed: 20045723]

[48]. Ralph SJ; Rodriguez-Enriquez S; Neuzil J; Saavedra E; Moreno-Sanchez R The causes of cancer revisited: mitochondrial malignancy and ROS-induced oncogenic transformation—why mitochondria are targets for cancer therapy. Mol. Aspects Med 31:145–170; 2010. [PubMed: 20206201]

[49]. Meitzler JL; Antony S; Wu Y; Juhasz A; Liu H; Jiang G; Lu J; Roy K; Doroshow JH NADPH oxidases: a perspective on reactive oxygen species production in tumor biology. Antioxid. Redox Signaling 20:2873–2889; 2014.

[50]. Thornber K; Colomba A; Ceccato L; Delsol G; Payrastre B; Gaits-Iacovoni F Reactive oxygen species and lipoxygenases regulate the oncogenicity of NPM-ALK-positive anaplastic large cell lymphomas. Oncogene 28:2690–2696; 2009. [PubMed: 19503098]

[51]. Zhang W; McQueen T; Schober W; Rassidakis G; Andreeff M; Konopleva M Leukotriene B4 receptor inhibitor LY293111 induces cell cycle arrest and apoptosis in human anaplastic large-cell lymphoma cells via JNK phosphorylation. Leukemia 19:1977–1984; 2005. [PubMed: 16151469]

[52]. Dikalov S Cross talk between mitochondria and NADPH oxidases. Free Radic. Biol. Med 51:1289–1301; 2011. [PubMed: 21777669]

[53]. Suto D; Sato K; Ohba Y; Yoshimura T; Fujii J Suppression of the proapoptotic function of cytochrome c by singlet oxygen via a haem redox state-independent mechanism. Biochem. J 392:399–406; 2005. [PubMed: 15966870]

[54]. Cho KJ; Seo JM; Kim JH Bioactive lipoxygenase metabolites stimulation of NADPH oxidases and reactive oxygen species. Mol. Cells 32:1–5; 2011. [PubMed: 21424583]

[55]. Chen F; Yu Y; Haigh S; Johnson J; Lucas R; Stepp DW; Fulton DJ Regulation of NADPH oxidase 5 by protein kinase C isoforms. PLoS One 9: e88405; 2014. [PubMed: 24505490]

[56]. Pandey D; Fulton DJ Molecular regulation of NADPH oxidase 5 via the MAPK pathway. Am. J. Physiol. Heart Circ. Physiol 300:H1336–1344; 2011. [PubMed: 21297032]

[57]. Orrenius S; Zhivotovsky B; Nicotera P Regulation of cell death: the calcium–apoptosis link. Nat. Rev. Mol. Cell Biol 4:552–565; 2003. [PubMed: 12838338]

[58]. Hubinger G; Scheffrahn I; Muller E; Bai R; Duyster J; Morris SW; Schrezenmeier H; Bergmann L The tyrosine kinase NPM-ALK, associated with anaplastic large cell lymphoma, binds the intracellular domain of the surface receptor CD30 but is not activated by CD30 stimulation. Exp. Hematol 27:1796–1805; 1999. [PubMed: 10641597]

[59]. Berridge MJ Inositol trisphosphate and calcium signalling. Nature 361:315–325; 1993. [PubMed: 8381210]

[60]. Rust R; Visser L; van der Leij J; Harms G; Blokzijl T; Deloulme JC; van der Vlies P; Kamps W; Kok K; Lim M; Poppema S; van den Berg A High expression of calcium-binding proteins, S100A10, S100A11 and CALM2 in anaplastic large cell lymphoma. Br. J. Haematol 131:596–608; 2005. [PubMed: 16351635]

[61]. Hallberg B; Palmer RH Mechanistic insight into ALK receptor tyrosine kinase in human cancer biology. Nat. Rev. Cancer 13:685–700; 2013. [PubMed: 24060861]

[62]. Sibon et al., JCO 2012.

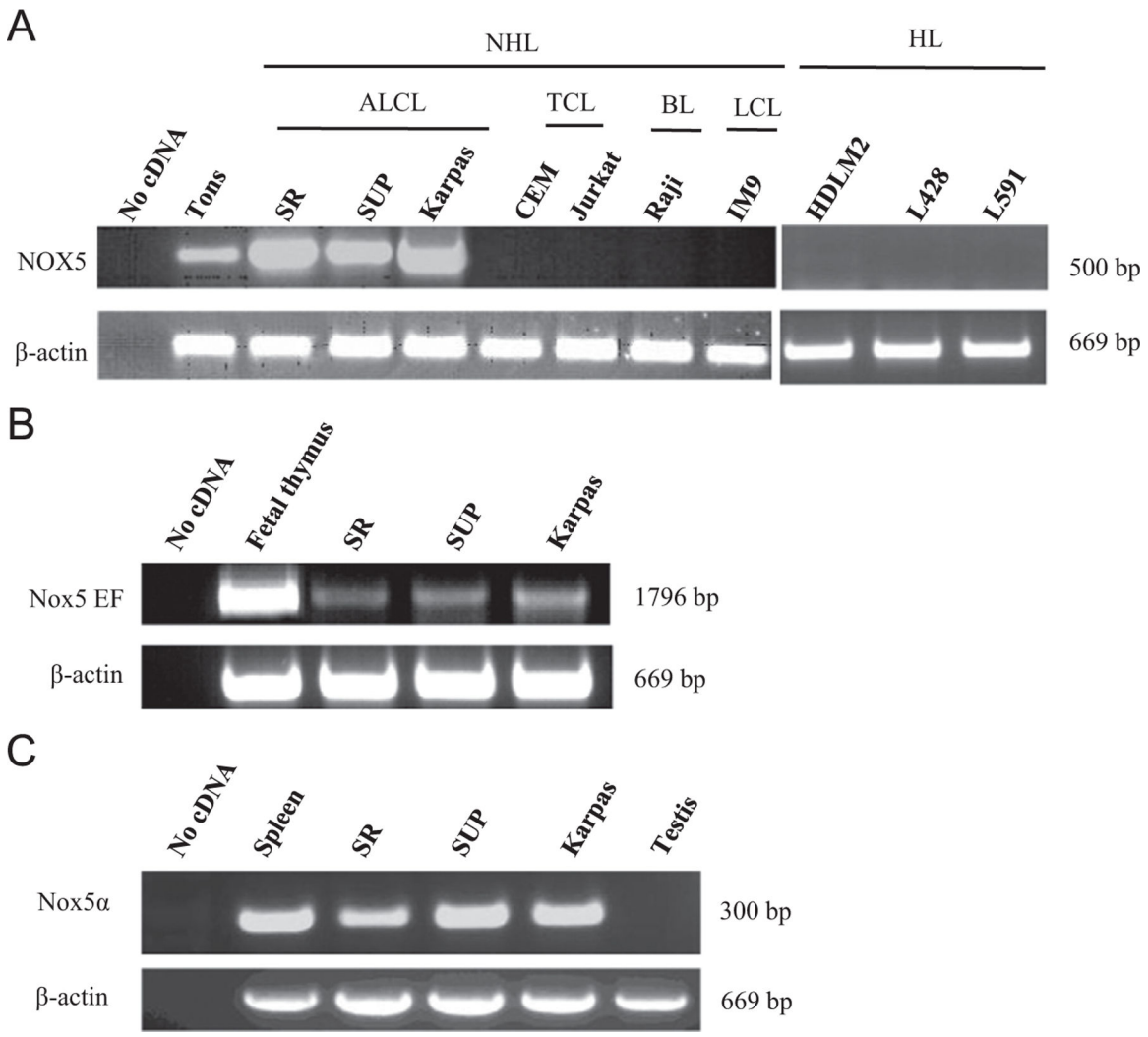

Fig. 1.

Unique expression of NOX5 in ALCL cell lines. (A) RT-PCR was performed for NOX5 on cDNAs derived from various lymphoma cell lines: non-Hodgkin (NHL) and Hodgkin (HL) types including anaplastic large-cell lymphoma (ALCL), T cell lymphoma (TCL), Burkitt lymphoma (BL), and large-cell lymphoma (LCL) cells. The bottom shows β-actin as loading control. No cDNA denotes PCR without preceding reverse transcription step. Human tonsil (Tons) cDNA was used as positive control. SR, SR-786 cell line; SUP, SUP-M2 cell line; Karpas, Karpas-299 cell line. (B) Presence of the mRNA segment coding for the activation domain of NOX5 in ALCL cells. Human fetal thymus cDNA was used as positive control. EF, the calcium-binding EF-hand domain. (C) Expression of the NOX5α isoform in ALCL cells. Human spleen cDNA was used as positive and human testis cDNA as negative control.

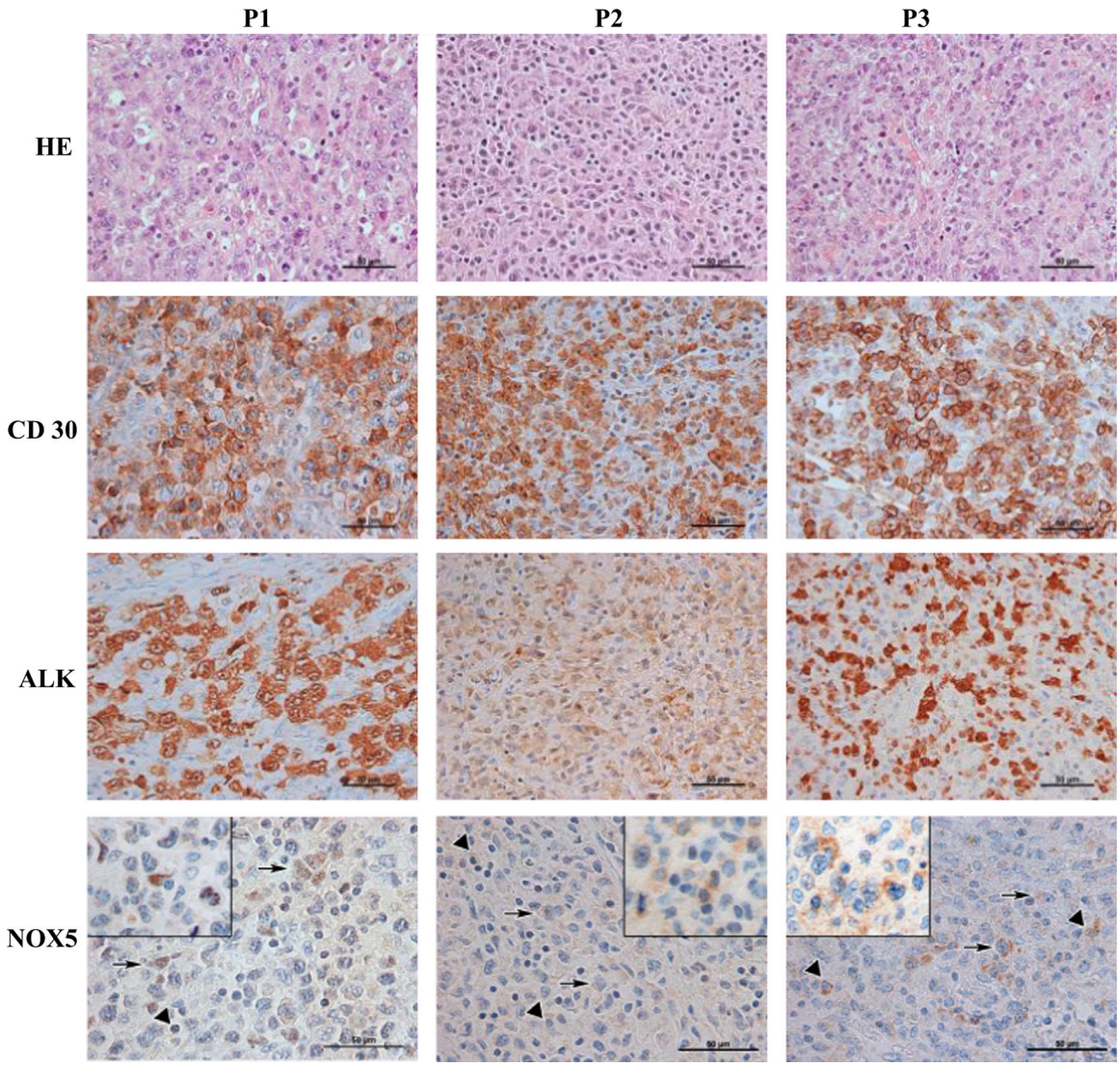

Fig. 2.

Immunohistochemical detection of NOX5 expression in pediatric ALK$^+$ ALCL tumor samples. Three pediatric ALK$^+$ ALCL tumoral samples were stained with hematoxylin–eosin or processed for immunohistochemical detection using CD30−, ALK−, or NOX5-specific antibodies. Triangles denote plasma cells, arrows point to tumor cells. P1, P2, P3, patient 1, patient 2, patient 3. Original magnification, 400 × (HE, CD30, and ALK) or 600 × (NOX5), with insets showing additional positive tumor cells at higher magnification.

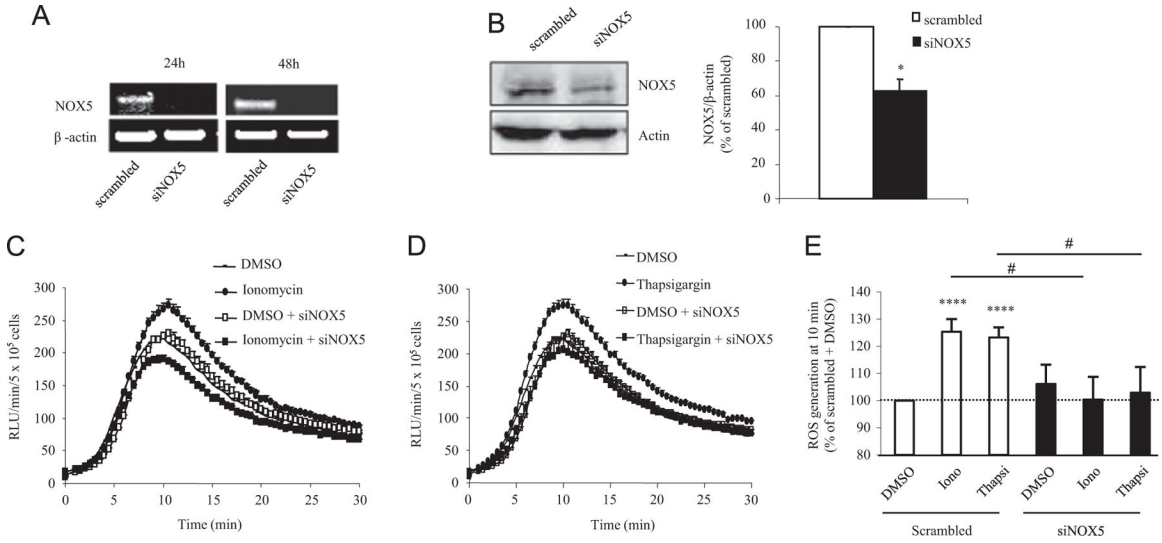

Fig. 3.

SiRNA-mediated NOX5 knockdown in Karpas-299 cells diminishes Ca^{2+}-induced ROS production. Karpas-299 cells were transfected with NOX5-specific (siNOX5) or scrambled siRNA. Experiments ($n = 4$) were carried out in triplicate for each condition. (A) RT-PCR detection of NOX5 and β-actin mRNAs. A representative image is shown. (B) Western blot analysis (left) and quantification (right) of NOX5 protein levels in Karpas-299 cells. Graph represents protein levels expressed as the percentage of the scrambled siRNA-transfected cells. *$p < 0.05$, scrambled vs siNOX5 siRNA-transfected cells. (C) Ionomycin- and (D) thapsigargin-induced ROS production measured as luminol oxidation in siNOX5 or scrambled siRNA-transfected Karpas-299 cells. The graphs show the amount of ROS (RLU/5 × 10^5 cells/min) released by Karpas-299 cells after ionomycin or thapsigargin addition at the 0-min time point. A representative experiment is shown. (E) Quantification of maximal induction of superoxide generation upon ionomycin and thapsigargin stimulation expressed as the percentage of stimulation obtained in the scrambled siRNA-transfected cells. Data are shown as the mean ± SEM and were obtained from six independent experiments. ****$p < 0.0001$, scrambled vs scrambled-transfected cells stimulated with ionomycin or thapsigargin, #$p < 0.01$, scrambled vs siNOX5 siRNA-transfected cells after ionomycin or thapsigargin stimulation.

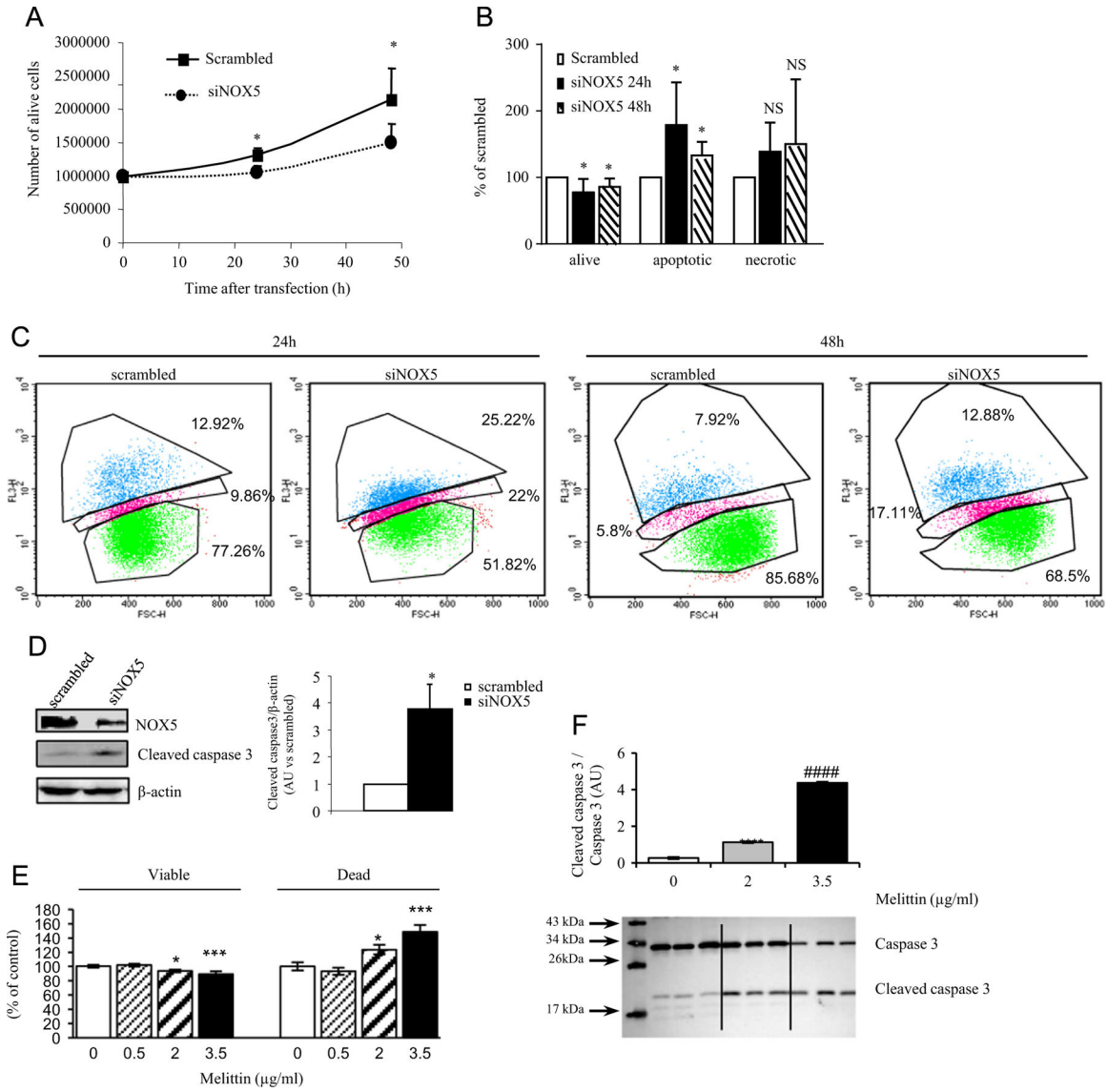

Fig. 4.

NOX5 depletion induces apoptosis. Karpas-299 cells were transfected with scrambled or NOX5-specific siRNA and were analyzed 24 and 48 h after transfection. (A) Number of live cells measured by trypan blue staining. *$p < 0.05$, scrambled vs siNOX5 siRNA-transfected cells; data are derived from four or five independent experiments. (B) Karpas-299 cells were stained with 7-AAD and apoptosis was determined by FACS analysis. Graph depicts live, apoptotic, and necrotic NOX5 siRNA-transfected cells expressed as a percentage of scrambled siRNA-transfected cells. Data are derived from four experiments, *$p < 0.01$ determined by Student's *t* test. (C) Representative FACS images of 7-AAD-stained scrambled and NOX5-specific siRNA-transfected cells after 24 and 48 h of transfection. Values marked are the percentage of cells in necrotic and apoptotic phase or alive (from top to bottom). (D) Western blot detection of NOX5 and cleaved caspase 3 in scrambled or NOX5-specific siRNA-transfected Karpas-299 48 h after transfection. β-Actin was used as loading control. Graph depicts quantification of cleaved caspase 3 levels in siNOX5-

transfected Karpas-299 cells relative to levels in scrambled siRNA-transfected cells. *$p <$ 0.01 determined by Student's *t* test. (E) Apoptosis upon melittin treatment. Graph depicts the live and apoptotic Karpas-299 cells determined by trypan blue exclusion upon treatment with 0.5, 2, and 3.5 μg/ml melittin after 72 h of treatment. Data are expressed as the percentage of control, DMSO-treated cells and are derived from two or three independent experiments conducted in triplicate for each condition. *$p < 0.05$ and ***$p < 0.001$, 2 and 3.5 μg/ml melittin vs DMSO-treated cells, respectively. (F) Detection and quantification of caspase 3 cleavage upon melittin treatment. Data are expressed as the mean ± SEM compared to DMSO-treated control cells. AU, arbitrary unit. ****$p < 0.0001$, melittin- vs DMSO-treated cells; ####$p < 0.0001$, 3.5 vs 2 μg/ml melittin-treated cells.

Table 1

Characteristics of ALCL patients and tumor biopsies.

Case	Diagnosis	Stage	Gender	Age	IHC	Cytogenetic analysis	Clinical course, months
1	ALCL	III	F	15 years	$CD30^+$, ALK^+, faint EMA^+, T cell markers –	t(2;5)(p23;q35); *NPM1/ALK*	CCR, 153
2	ALCL	III	M	3 years	$CD30^+$, less intense ALK^+, EMA, focal $CD3^+$	NA	CR, 24, R
3	ALCL	III	F	7.5 months	$CD30^+$, ALK^+, focal $CD4^+$, rare $CD3^+$	NA	CCR, 168

IHC, immunohistochemistry; NA, not available; CR, complete remission; R, relapse; CCR, continuous complete remission.